Journal of ETA Maritime Science 2024;12(1):14-24

Investigation of Scale Effects on Linear Vertical Maneuvering Derivatives of a Submarine

Emre Kahramanoğlu[1], Savaş Sezen[2], Ferdi Çakıcı[3]

[1]İstanbul Technical University Faculty of Maritime, Department of Marine Engineering, İstanbul, Türkiye
[2]Lloyd's Register EMEA, Southampton, United Kingdom
[3]Yıldız Technical University Naval Architecture and Maritime Faculty, Department of Naval Architecture and Marine Engineering, İstanbul, Türkiye

Abstract

This paper aims to show the scale effects of vertical maneuvering derivatives for an underwater vehicle using computational fluid dynamics (CFD). The model scale and full-scale benchmark DARPA suboff hull forms were used in numerical vertical planar motion mechanism simulations to achieve this aim. The heave forces, pitch moments, and Euler coefficients are calculated together with the linear vertical maneuvering derivatives by implementing the Fourier series expansion approach. The results show that the coupled added mass terms are significantly influenced by the scale effects, whereas the impact of scale effects on the decoupled added mass and coupled and decoupled damping terms is negligible. Considering that the effects of the coupled added mass on the vertical maneuvering characteristics are almost negligible, the vertical maneuvering of a submarine is slightly influenced by the scale effects.

Keywords: Submarine, Vertical maneuvering derivatives, Scale effect, CFD

1. Introduction

Having an effective horizontal maneuvering capability is essential for naval submarines because of rapid location and direction change requirements in case of emergencies. However, underwater vehicles can move in 6DOF motions in deep water, and thus, they may need to reach the free surface rapidly to escape hostile attacks, flooding, etc. Therefore, they should have good horizontal and vertical maneuvering capabilities. Two different approaches are generally used to understand the maneuvering behavior of an underwater vehicle or surface vessel. The first is free-running tests, where the vehicle can move freely in an experimental or numerical tank. Although this approach is considered to be the most accurate approach for calculating the maneuvering behavior of a vehicle, it is rather expensive and challenging due to constraints in facilities and numerical solvers. Therefore, as an alternative to this approach, simulation-based methods can be used to determine maneuvering characteristics. In this method, the maneuvering derivatives of a vehicle can be calculated using different mechanisms, such as planar motion mechanism, rotating arm, static drift, circular motion technique. To use the derivatives obtained from numerical or experimental techniques, a mathematical model is required.

1.1. Literature Review

The mathematical model for surface ships was first proposed by Davidson and Schiff [1] and then developed by Abkowitz [2]. Gertler and Hagen [3] also proposed a mathematical model to represent the maneuvering motion of an underwater vehicle for the first time, and this model was further modified by Feldman [4] with crossflow corrections.

The Defense Advanced Research Projects Agency (DARPA) Suboff is one of the most used benchmark underwater vehicle models in the literature. Comprehensive captive model experiments of DARPA were conducted by Roddy [5], and different techniques were used to obtain the maneuvering derivatives in horizontal and vertical planes during the experiments. Following this, Lin et al. [6] and

Address for Correspondence: Emre Kahramanoğlu, İstanbul Technical University Faculty of Maritime, Department of Marine Engineering, İstanbul, Türkiye
E-mail: emrekahramanoglu@gmail.com
ORCID ID: orcid.org/0000-0002-3646-1170

Received: 12.09.2023
Last Revision Received: 14.11.2023
Accepted: 12.12.2023

To cite this article: E. Kahramanoğlu, S. Sezen, and F. Çakıcı. "Investigation of Scale Effects on Linear Vertical Maneuvering Derivatives of a Submarine." *Journal of ETA Maritime Science*, vol. 12(1), pp. 14-24, 2024.

Xiaoyang et al. [7] conducted systematic experiments using the same DARPA Suboff hull form with another scale ratio. The results were compared with the experimental data obtained by Roddy [5]. The experiments performed by Roddy [5] mainly focused on horizontal maneuvering derivatives, whereas the vertical maneuvering derivatives were of great interest for the experiments performed by Lin et al. [6] and Xiaoyang et al. [7]. In another experimental study of DARPA Suboff, the effect of immersion on course-keeping stability was investigated by Efremov and Milanov [8]. They showed that the hydrodynamic derivatives change with immersion and highlighted that the change in derivatives with immersion could cause the loss of course stability of the submarine.

To obtain the horizontal and vertical derivatives, a series of tests were conducted in different facilities for two different model scales of DARPA Suboff, as shown in Table 1.

With the development of numerical techniques, computational fluid dynamics techniques are becoming appealing for calculating the maneuvering characteristics of vessels, similar to other hydrodynamic performance predictions (e.g., Budak and Beji [9], Sezen et al. [10], Sezen et al. [11], Dogrul [12]). In this regard, Table 2a summarizes the studies solely focused on the prediction of horizontal and vertical maneuvering of the DARPA Suboff. Additionally, Table 2b shows the other numerical studies performed using other underwater vehicles. The approaches for predicting the hydrodynamic derivatives are also shown in Table 2a and Table 2b.

Table 1. *Experimental studies of the DARPA Suboff*

	Model scale	Static drift	Pure sway	Pure yaw	Pure heave	Pure pitch
Roddy [5]	1/24	+	+	+	+	+
Lin et al. [6]	1/48	+	+	+	-	-
Efremov and Milanov [8]	1/24	+	-	+	-	-
Xiaoyang et al. [7]	1/48	+	-	-	+	+

Table 2a*. Numerical studies on the maneuvering of DARPA Suboff*

		Static Drift	Rotating Arm	Pure Sway	Pure Yaw	Pure Heave	Pure Pitch	Direct Modelling
Vaz et al. [13]	DARPA	+	-	-	-	-	+	-
Drouet et al. [14]	DARPA	+	-	-	-	-	-	-
Pan et al. [15]	DARPA	+	-	+	+	+	+	-
Zhang et al. [16]	DRDC STR, DARPA, Series 58	-	+	-	-	-	-	-
Can [17]	DARPA, Autosub	+	+	-	-	+	+	-
Duman et al. [18]	DARPA	+	-	-	-	-	-	-
Feng et al. [19]	DARPA	-	-	-	-	-	-	+
Foroushani and Sabzpooshani [20]	DARPA	-	-	+	+	+	+	-
Delen and Kinaci [21]	DARPA	-	-	-	-	-	-	+
Kahramanoglu [22]	DARPA	-	-	+	+	-	-	-
Zhao et al. [23]	DARPA	+	+	-	-	-	-	-
Öztürk et al. [24]	DARPA	+	-	-	-	-	-	-

Table 2b*. Numerical studies on the maneuvering of other underwater vehicles*

	Submarine Model	Static Drift	Rotating Arm	Pure Sway	Pure Yaw	Pure Heave	Pure Pitch	Direct Modelling
Tyagi and Sen [25]	Kempf, Blue Eyes	+	-	-	-	-	-	-
Phillips et al. [26]	Autosub	+	+	-	-	-	-	-
Fureby et al. [27]	DTSO	+	-	-	-	-	-	-
Carrica et al. [28]	Joubert BB2	-	-	-	-	-	-	+
Carrica et al. [29]	Joubert BB2	-	-	-	-	-	-	+
Dubbioso et al. [30]	CNR Insean 2475	-	-	-	-	-	-	+
Nguyen et al. [31]	Self-built	+	+	-	-	-	-	-
Kim et al. [32]	Joubert BB2	-	-	-	-	-	-	+
Zhang et al. [33]	Self-built	-	-	-	-	-	-	+
Doyle et al. [34]	Phoenix	+	-	+	-	-	-	-
Cho et al. [35]	Joubert BB2	+	-	+	+	+	+	-
Han et al. [36]	BB2	-	-	-	-	-	-	+

As summarized above, several studies have investigated horizontal and vertical maneuvering derivatives using numerical and experimental methods on a model scale. As the aim of these investigations is to predict the maneuvering performance of underwater vehicles on a full scale, the coefficients calculated by simulation-based approaches can be greatly influenced by the scale effects. Hence, this might result in a misprediction of the maneuvering performance of underwater vehicles. To the best of the authors' knowledge, there is a research gap in investigating the scale effects on the vertical maneuvering performance of underwater vehicles in the open literature. Therefore, this study aims to explore the scale effects on the vertical maneuvering performance of underwater vehicles. To achieve this aim, two different scales (i.e., model and full-scale) were used in the CFD calculations.

1.2. Aim of the Study

In the leading author's recent study [22], the scale effects on horizontal maneuvering performance were comprehensively investigated using the same benchmark submarine model. This study is a continuation of the recently published study of the leading author [22] by expanding the investigations of scale effects for vertical maneuvering derivatives for the first time in the literature. This paper is organized as follows. Section 2 describes the mathematical model, including the submarine geometry and the physical model. The numerical results are given in Section 3, and the concluding remarks are presented in the last section.

2. Solution Strategy

2.1. Submarine Geometry

The DARPA Suboff model was used in this study. The fully appended submarine form (AFF-8) apart from the wing ring was selected. The 3D geometry of the underwater vehicle is shown in Figure 1. The main properties are given in Table 3 for both scales.

Figure 1. *The submarine geometry used in the present study*

2.2. Equation of Motions

In this study, only pure heaving and pitching motions were considered at a certain surge speed. All simulations were conducted at 3DOF, and the equations of these motions can be derived from Newton's second law, similar to the study of Xiaoyang et al. [7], and written by following the notations explained in SNAME [37]:

$$X = m\left[\dot{u} + wq - x_G q^2 + z_G \dot{q}\right] \quad (1)$$

$$Z = m\left[\dot{w} - uq - z_G q^2 - x_G \dot{q}\right] \quad (2)$$

$$M = I_{YY}\dot{q} + m\left[z_G(\dot{u} + wq) - x_G(\dot{w} - uq)\right] \quad (3)$$

Equations (1-3) represent the surge, heave, and pitch motions, respectively. I_{YY} depicts the moment of inertia for pitch direction while x_G and z_G depict the longitudinal and vertical centers of gravity. u, w and q depict the surge, heave and pitch velocities, respectively, while the dotted terms represent the acceleration. M denotes the pitch moment, while X and Z denote the surge and heave forces, respectively. Although these terms might be due to waves, propeller, hydrostatic, and hydrodynamic loads, this paper focuses only on the term associated with hydrodynamics. Because only the linear terms are taken into consideration, the hydrodynamic loads for heave and pitch motions can be represented as follows, where Z_H and M_H represent the hydrodynamic force in the Z direction and the hydrodynamic moment around the Y axis:

$$Z_H = Z_w w + Z_{\dot{w}} \dot{w} + Z_q q + Z_{\dot{q}} \dot{q} \quad (4)$$

$$M_H = M_w w + M_{\dot{w}} \dot{w} + M_q q + M_{\dot{q}} \dot{q} \quad (5)$$

Table 3. *Main properties of the underwater vehicle*

Main Particular	Unit	λ = 1/24 (Model scale)	λ = 1/1 (Full scale)
Length Overall (L_{OA})	m	4.356	104.54
Length between perpendiculars (L_{PP})	m	4.261	102.26
Maximum Diameter (D_{MAX})	m	0.508	12.192
Displacement (Δ)	tons	0.704	9729.7
Froude Number (Fn)	-	0.515	0.515
Reynolds Number (Rn)	-	$1.4\ 10^7$	$1.7\ 10^9$

Where Z_w and Z_q denote the damping terms in the z-direction due to the heave and pitch velocities, respectively, while the dot products ($Z_{\dot{w}}$ and $Z_{\dot{q}}$) denote the added mass terms due to the heave and pitch acceleration. M_w and M_q represent the damping terms around the y-axis due to heave and pitch velocities, respectively, while the dot products ($M_{\dot{w}}$ and $M_{\dot{q}}$) represent the acceleration terms due to the heave and pitch acceleration around the y-axis.

2.3. Numerical Modeling

2.3.1. Boundary conditions and computational domain

Similar to the recent study of the leading author [22], a computational domain was used to solve the flow around the submarines. The computational domain size was selected according to the ITTC guidelines [38] to avoid potential reflections from the boundaries, as shown in Figure 2. The depth and breadth of the computational domain extends to 4L. Here, the right side of the computational domain was selected as the velocity inlet, while the left side was selected as the pressure outlet. The other boundaries of the computational domain were also defined as the velocity inlet. To satisfy the kinematic boundary conditions, the submarine geometry was defined as a no-slip wall.

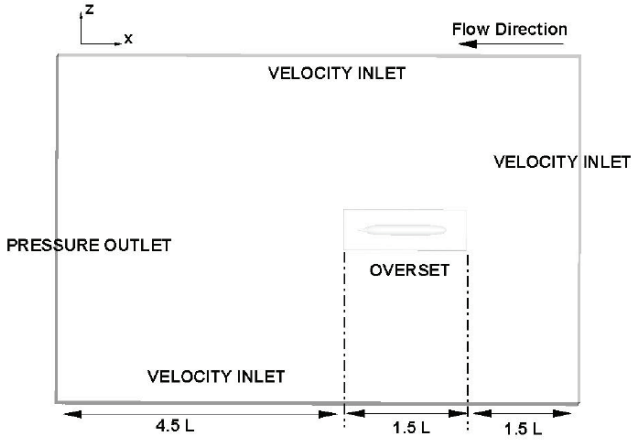

Figure 2. *Sizes of the domain and boundaries*

2.3.2. Meshing strategy and physical modeling

The overset mesh technique was used to accurately model the flow field around the model and full-scale forms. To accurately transfer the information from the overset zone to the static background, the grid structure was enlarged systematically, and the mesh transition was kept as smooth as possible between the background and overset regions. The mesh structure around the submarine hull is shown in Figure 3.

In the CFD simulations, the unsteady RANS method, the k-ω SST turbulence model, and all y+ treatment methods were utilized in a manner similar to the studies in the literature [10,11,22]. To discretize the temporal and convectional terms, a second-order upwind scheme was used. Because the maneuvering motion was modeled in 3DOF, the submarine form was forced only for vertical motion by maintaining a certain surge speed in the CFD simulations.

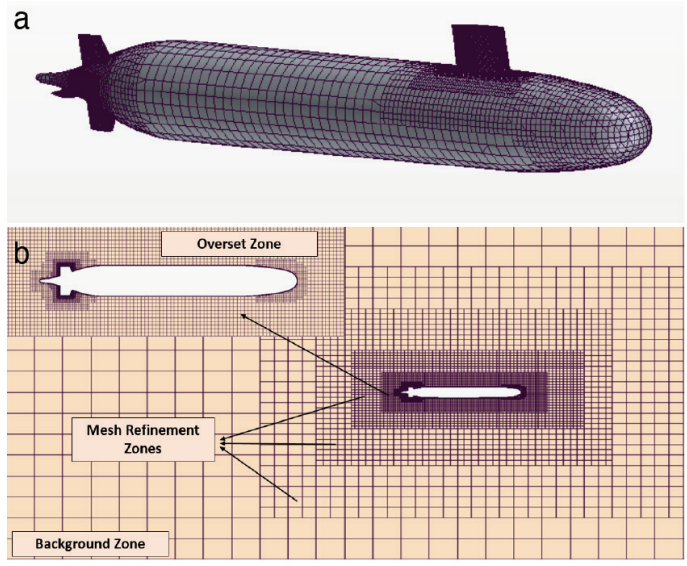

Figure 3. *a) Mesh structure on underwater vehicles. b) Mesh structure of the domain*

3. Results

In this study, pure heave and pure pitch analyses were performed to calculate the vertical maneuvering derivatives for a benchmark submarine, the DARPA Suboff. Thus, the test matrix given in Table 4 was created considering the ITTC recommendations [39] and previous studies in the literature [20,22]. Note that these cases are for the model scale and full scale of DARPA Suboff. In total, there are 16 cases investigated in this study.

The forces, moments, and rotational and translational velocities/accelerations were non-dimensionalized, similar

Table 4a*. Test matrix for pure heaving*

Test No	Heave Amplitude/ L_{pp} [-]	Frequency*L_{pp}/V [-]	w/V [-]
H1	0.0271	1.6630	0.0450
H2	0.0361	1.6630	0.0600
H3	0.0542	1.6630	0.0901
H4	0.0812	1.6630	0.1351

Table 4b*. Test matrix for pure pitching*

Test No	Heave Amplitude/ L_{pp} [-]	Frequency*L_{pp}/V [-]	q*L_{pp}/V [-]
P1	0.0162	2.8142	0.1279
P2	0.0242	2.8142	0.1919
P3	0.0323	2.8142	0.2558
P4	0.0485	2.8142	0.3838

to the findings of the leading author's recent study [22]. The heave force and the pitch moment values were non-dimensionalized by the following equations:

$$Z' = Z/(0.5\rho L^2 V^2) \quad (6)$$

$$M' = M/(0.5\rho L^3 V^2) \quad (7)$$

After calculating the time series of non-dimensional forces and moments, they were defined by applying Fourier series expansion following the methodology given in Equation (8) and Equation (15):

$$Z'(t) = Z'_{cos}\cos(\omega t) + Z'_{sin}\sin(\omega t) \quad (8)$$

$$M'(t) = M'_{cos}\cos(\omega t) + M'_{sin}\sin(\omega t) \quad (9)$$

$$Z'_{cos} = \frac{2}{T}\int 0\ T\ Z'(t)\cos(\omega t)dt \quad (10)$$

$$Z'_{sin} = \frac{2}{T}\int 0\ T\ Z'(t)\sin(\omega t)dt \quad (11)$$

$$M'_{cos} = \frac{2}{T}\int 0\ T\ M'(t)\cos(\omega t)dt \quad (12)$$

$$M'_{cos} = \frac{2}{T}\int 0\ T\ M'(t)\cos(\omega t)dt \quad (13)$$

$$\beta_Z = \arctan\left(\frac{Z_{cos}}{Z_{sin}}\right) \quad (14)$$

$$\beta_M = \arctan\left(\frac{M_{cos}}{M_{sin}}\right) \quad (15)$$

3.1. Uncertainty Analyses

The uncertainty assessment of the present study was conducted by implementing the Grid Convergence Index) method that was proposed by Roache [40] and developed with many studies [41,42]. Similar to previous studies conducted by authors on both surface vessels [43] and underwater vehicles [11,22], the methodology suggested by Celik et al. [44] was used for calculating the temporal and spatial uncertainty.

The H2 test case, shown in Table 4a, was selected to obtain the total uncertainty for the amplitude of the pitch moment obtained from the pure heaving analyses. The convergence of the scalar values and the uncertainty of the numerical solution are given in Figure 4 and Table 5, respectively. It can be understood from Figure 4 that the

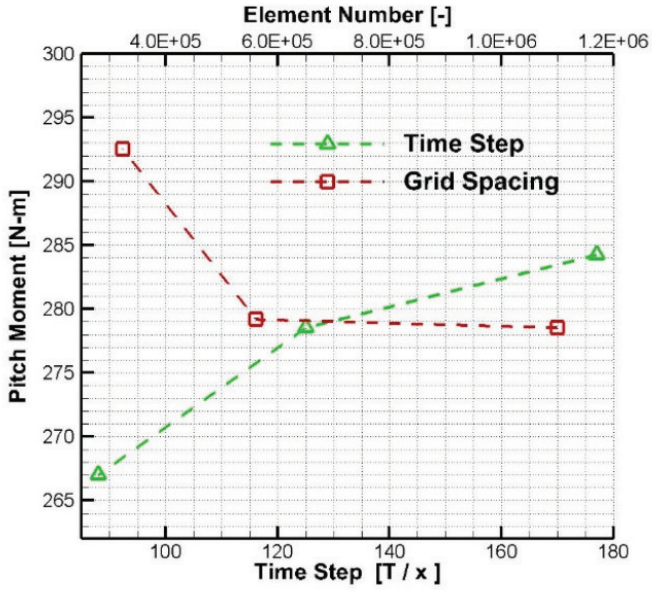

Figure 4. *Convergence of pitch moments*

pitch moment values converge to a scalar value as the number of elements increases or as the time step size decreases. Based on the uncertainty study, a fine grid was selected for CFD simulations. As the difference between the fine and medium time-step sizes is small, the medium time-step size was selected to reduce the computational cost of CFD simulations. In Table 5, T denotes the period of the heave motion, U denotes the uncertainty, R denotes the convergence factor, and r denotes the refinement factor, which was kept constant in all analyses.

3.2. Pure Heaving

Before presenting all numerical data, the obtained results from the numerical method are compared with those presented in the literature. If the moment and forces obtained from different test cases are fitted to a one-degree polynomial, as explained by Yoon et al. [45], the maneuvering derivatives in accordance with the added mass and damping terms can be calculated. A comparison of the maneuvering derivatives is presented in Table 6. According to the results listed in Table 6, there are some differences between the present study and other results

Table 5. *Uncertainty results*

	Element number [-]	Pitch moment [N-m]	Time step size [s]	Pitch moment [N-m]
Fine	1.10 x 10^6	278.54	T/177	284.26
Medium	5.62 x 10^5	279.19	T/125	278.54
Coarse	3.24 x 10^5	292.54	T/88	267.00
R	0.0490		0.4954	
r	1.4142		1.4142	
%U	0.02%		2.47%	
Total uncertainty () = = 2.47 %				

Table 6. *Comparison of derivatives obtained from pure heaving*

	Present study	Roddy (EFD) [5]	Foroushani and Sabzpooshani (CFD) [20]	Zhao et al. (CFD) [23]	Pan et al. (CFD) [15]	Liang et al. (EFD) [7]
Z_w	-0.01736	-0.01391	-0.01468	-0.01331	-0.01570	-0.03560
Z_w	-0.01882	-0.01453	-0.01753	-	-0.01811	-0.01010
M_w	0.01035	0.01032	0.01057	0.01104	0.01009	0.01172
M_w	-0.00622	-0.00056	-0.00080	-	-0.00063	0.00106

presented in the literature. These discrepancies can arise from differences in measurement techniques, the method used to obtain maneuvering derivatives, and variations in experimental condition. Although there are some acceptable differences, the numerical derivatives obtained from the present numerical method generally match well with the results presented in the literature.

Following the validation of the numerical results with experimental and numerical studies in the literature, the scale effects on forces, moments, phases, and derivatives can be investigated in detail. As stated before, pure heaving simulations were conducted using the test cases explained in Table 4, while the Froude number of both scales was kept the same as 0.515. In this simulation, the submarine only heaved; thus, the pitch velocity and pitch acceleration were equal to zero in Equation (4) and Equation (5). Then, the forces and moments, which are functions of only heave velocity and heave acceleration, were decomposed using the Fourier series expansion approach.

In Figure 5, the heave forces in terms of different heave velocities are presented for both scales. According to this figure, the coefficients associated with the cosine term (ZC') for full scale are higher than those of the model scale values. In contrast, the coefficients related to the sinus term (ZS') are lower for all heave velocities in full-scale than the values in the model scale. Only a slight difference in the amplitudes (Z') of both scales is observed over several heave velocities. When the phase of the heave forces is examined, there is a significant difference, especially at lower heave velocities. These differences in phases cause differentiation in the Euler components of the heave force.

In Figure 6, the pitch moments obtained from pure heaving analyses are compared for both scales in terms of different heave velocities. According to Figure 6, the pitch moment amplitudes are similar for both scales, whereas the amplitudes of the full scale are slightly lower than that of the model scale. Although the Euler coefficients related

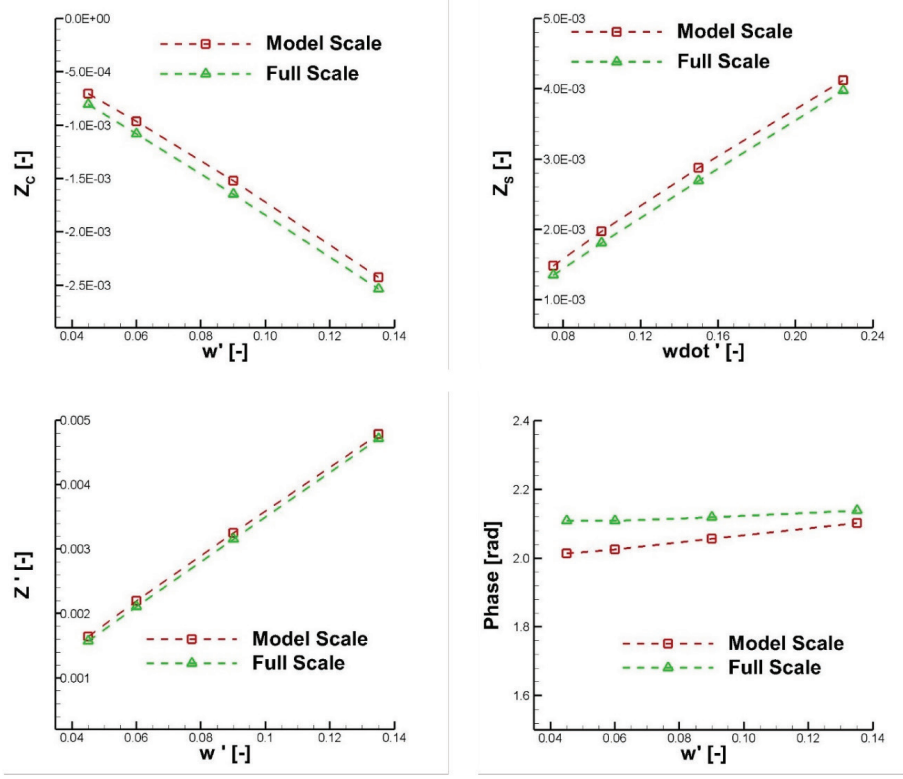

Figure 5. *Heave force, Euler components, and phases in terms of different heave velocities*

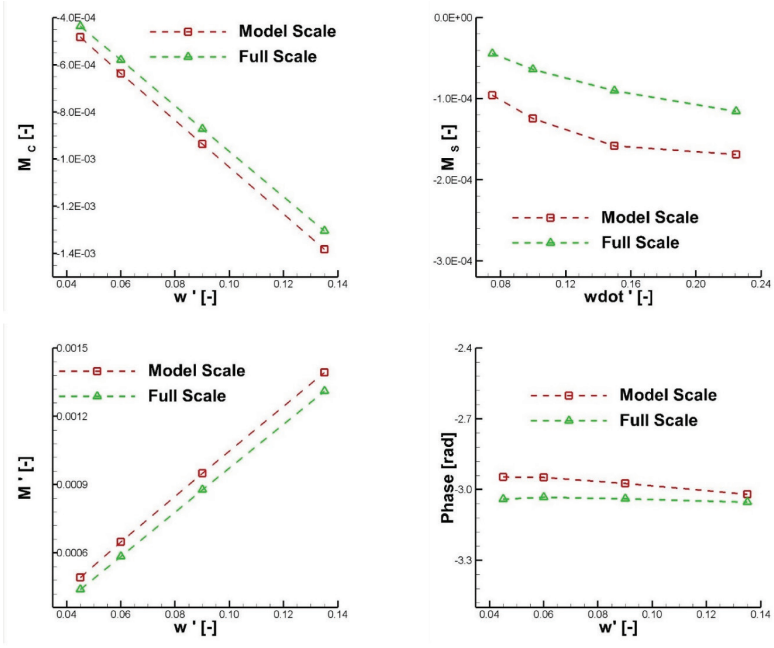

Figure 6. *Pitch moment, Euler components, and phases in terms of different heave velocities*

to the cosine term (M_C') for the model scale are higher, the trend of the general curve of both scales is similar. However, the Euler coefficients related to the sinus term (M_S') for the model scale are higher than those for the full scale. Similar to Figure 5, there is a discrepancy in the phases for both scales.

Table 7 lists the derivatives obtained from the pure heaving simulations for both scales. As underlined before, the methodology presented by Yoon et al. [45] was followed to calculate the maneuvering derivatives. As expected from the data shown in Figure 5, the derivatives for both scales are very similar for Z_w and $Z_{\dot{w}}$. Similarly, M_w values are similar for both models because the slopes of the pitch moment component related to cosine (M_C') are very similar.

Table 7. *Maneuvering derivatives obtained from the pure heaving analyses*

Derivative	Model	Full
Z_w	-0.01736	-0.01853
$Z_{\dot{w}}$	-0.01882	-0.01782
M_w	0.01035	0.00965
$M_{\dot{w}}$	-0.00622	-0.00055

However, contrary to $M_{\dot{w}}$, the value of M_w are greatly influenced by the scale effects. When the data are examined, it is understood that a considerable difference in the coupled added mass occurs because of the phase difference.

3.3. Pure Pitching

The numerical results for the model scale are compared with numerical and/or experimental results presented in the literature in Table 8.

As given in Table 8, the derivatives for the heave force (Z) are generally under predicted, whereas the derivatives related to pitch moment (M) are in good agreement with the derivatives obtained from the literature. The difference in the heave forces was also observed in a previous study [22]. This difference can be associated with the wing ring, which was not modeled in the present study, unlike some other studies. In addition, the numerical parameters selected in this study can also be associated with the difference between the current and other numerical studies.

Similar to the pure heaving analyses, pure pitching analyses were conducted at the same Froude number for both scales according to the test cases listed in Table 4b. Unlike the previous simulation, the heave velocities and

Table 8. *Comparison of derivatives obtained from pure pitching*

	Present study	Roddy (EFD) [5]	Foroushani and Sabzpooshani (CFD) [20]	Zhao et al. (EFD) [46]	Pan et al. (CFD) [15]	Liang et al. (EFD) [7]
Z_q	-0.00484	-0.00755	-0.00682	-0.00796	-0.00778	-0.00164
$Z_{\dot{q}}$	-0.00018	-0.00063	-0.00058	-	-0.00063	-0.00102
M_q	-0.00278	-0.00370	-0.00317	-0.00397	-0.00347	-0.00289
$M_{\dot{q}}$	-0.00094	-0.00086	-0.00102	-	-0.00095	-0.00076

acceleration were set to zero because the underwater vehicle was only forced to perform pitch motion. Therefore, the heave force and pitch moment are considered to be functions of pitch velocity and pitch acceleration in Equation (4) and Equation (5).

The heave forces obtained from the pure pitching analyses in terms of different pitch velocities are shown in Figure 7. The amplitudes (Z') for the model scale are lower than those for the full-scale results, similar to the coefficient related to sinus (Z_S'). Considering the coefficients related to cosine (Z_C'), the sign of the full-scale results changes with different pitch velocities. Although the general trend of the curve is similar for both scales for the amplitudes and the component related to sinus, there is a clear offset between them. Similar to these terms, the phases of different scales show some discrepancies, especially for lower pitch velocities. Thus, the differences in the components are caused by differences in the amplitudes and phases.

In Figure 8, the pitch moments obtained from the different pitch velocities are shown for both scales. According to this figure, the amplitudes of both scales are almost the same for all pitch velocity ranges. The coefficients related to the

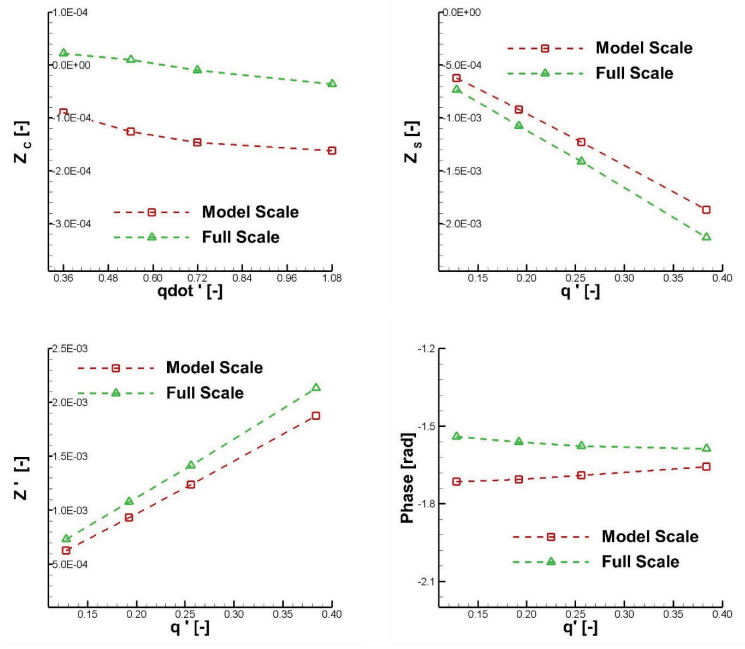

Figure 7. *Heave forces, Euler components, and phases in terms of pitch velocities*

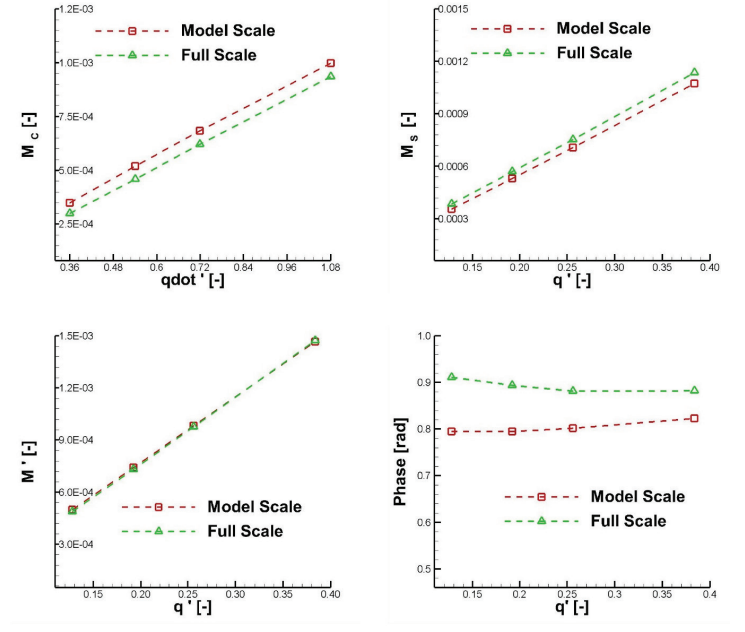

Figure 8. *Heave forces, Euler components, and phases in terms of pitch velocities*

sinus term (M_S') for the model scale are slightly lower than the full-scale results, although the full-scale results for the coefficients related to cosine (M_C') are slightly lower than the model-scale results. The main difference for the Euler components appears to originate from the phase differences for both scales.

The derivatives obtained from the data shown in Figures 7 and 8 are listed in Table 9 for both scales. It should be noted that similar to pure heaving, the derivatives were calculated by fitting a linear curve by following the methodology presented by Yoon et al. [45]. As expected from the data shown in Figure 8, the derivatives related to pitch moments are similar for both scales (M_q and $M_{\dot{q}}$) since these derivatives directly are obtained from the slope of the fitted curves. It can be seen that Z_q values are very close for both models in Table 9, while the value of $Z_{\dot{q}}$ is greatly influenced by the scale effects. The main reason for this is the phase difference observed in the time domain data as well as the difference in the heave force amplitudes obtained from pure pitching analyses (see Figure 7).

Table 9. *Maneuvering derivatives obtained from the pure pitching analyses*

Derivative	Model scale	Full scale
Z_q	-0.00484	-0.00556
$Z_{\dot{q}}$	-0.00018	-0.00002
M_q	-0.00278	-0.00297
$M_{\dot{q}}$	-0.00094	-0.00086

4. Conclusion

In this study, the scale effects on the vertical maneuvering derivatives of a benchmark underwater vehicle were numerically investigated. Pure heaving and pure pitching simulations were conducted for two scales, and the linear vertical maneuvering derivatives were calculated, validated, and compared.

The following outcomes can be summarized as follows:

• The amplitudes of the heave force in pure heaving simulations are slightly affected by the scale effects. The scale effects can be considered negligible for damping (Z_w) and added mass term ($Z_{\dot{w}}$) of the heave force obtained from the pure heaving simulations.

• A pronounced scale effect on pure heaving simulations is found for the cross-coupled added mass term ($M_{\dot{w}}$), whereas the damping term of pitch moment (M_w) are not influenced by the scale effects.

• The scale effects on the pitch moment obtained from the pure pitching simulations are negligible. While there is a phase difference between both scales, this difference doesnot remarkably influence neither damping (M_q) nor added mass term ($M_{\dot{q}}$) of the pitch moment.

• Significant scale effects on the amplitudes were found for the heave force obtained from the pure pitching simulations.

• In addition to the differences in the amplitudes, the phases of the heave force in pure pitching change with scale. Thus, this can cause a remarkable difference in the derivatives, especially for the added mass term ($Z_{\dot{q}}$).

• The damping term of the heave force (Z_q) on pure pitching simulations is considerably affected (i.e., approximately 15%) compared with the cross-coupled damping term (M_w) obtained from pure heaving simulations.

• The main reason for the scale effects appears to be the phase differences between the different scales.

• The scale effect is more pronounced for the cross-coupled added mass terms, similar to the horizontal maneuvering results obtained from the leading author's recent study. Nevertheless, it is expected that the change in the cross-coupled added mass term with the scale ratio should not influence the overall maneuvering performance of the submarine. This is because the contributions of these terms to heave force and pitch moment are rather small.

This study is the second part of ongoing research on predicting the maneuvering performance of the submarine hull form at full scale using direct CFD simulations. Therefore, the authors are currently expanding their research in this field and comparing the results of direct CFD and system-based approaches for full-scale submarine hulls.

Authorship Contributions

Concept design: E. Kahramanoğlu, S. Sezen, and F. Çakıcı, Data Collection or Processing: E. Kahramanoğlu, S. Sezen, and F. Çakıcı, Analysis or Interpretation: E. Kahramanoğlu, S. Sezen, and F. Çakıcı, Literature Review: E. Kahramanoğlu, S. Sezen, and F. Çakıcı, Writing, Reviewing and Editing: E. Kahramanoğlu, S. Sezen, and F. Çakıcı.

Funding: The authors received no financial support for the research, authorship, and/or publication of this article.

References

[1] K. S. M. Davidson, and L. I. Schiff, "Turning and course keeping qualities." *Transactions - The Society of Naval Architects and Marine Engineers,* vol. 54, 1946.

[2] M. A. Abkowitz, *Lectures on Ship Hydrodynamics Steering and Maneuverability.* Technical Report. Hydro and Aerodynamic Laboratory, Lyngby, Denmark. Technical Report Hy-5. 1964.

[3] M. Gertler, and G. Hagen, *Standard Equations of Motion for Submarine Simulation.* Technical Report AD653861, June, 1967.

[4] J. Feldman, DTNSRDC Revised Standard Submarine Equations of Motion. David Taylor Research Center, Ship Performance Department (June), 1979.

[5] R. F. Roddy, Investigation of the Stability and Control Characteristics of Several Configurations of the DARPA Suboff Model (DTRC Model 5470) from Captive Model Experiments. David Taylor Research Center, Departmental Report DTRC/SHD-1298- 08 (September), 1990.

[6] Y. H. Lin, S. H. Tseng, and Y. H. Chen, "The experimental study on maneuvering derivatives of a submerged body SUBOFF by implementing the Planar Motion Mechanism tests." *Ocean Engineering,* vol. 170, pp. 120-135, Dec 2018.

[7] X. Liang, N. Ma, H. Liu, and X. Gu, "Experimental study on the maneuvering derivatives of a half-scale SUBOFF model in the vertical plane." *Ocean Engineering,* vol. 233, pp. 109052, Aug 2021.

[8] D. V. Efremov, and E. M. Milanov, "Hydrodynamics of DARPA SUBOFF submarine at shallowly immersion conditions." *TransNav, the International Journal on Marine Navigation and Safety of Sea Transportation,* vol. 13, pp. 337-342, 2019.

[9] G. Budak, and S. Beji, "Computational resistance analyses of a generic submarine hull form and its geometric variants." *Jounal of Ocean Techonology,* vol. 11, pp. 77-86, Jul 2016

[10] S. Sezen, C. Delen, A. Dogrul, and M. Atlar, "An investigation of scale effects on the self-propulsion characteristics of a submarine." *Applied Ocean Research,* vol. 113, pp. 102728, Aug 2021.

[11] S. Sezen, A. Dogrul, C. Delen, and S. Bal, "Investigation of self-propulsion of DARPA Suboff by RANS method." *Ocean Engineering,* vol. 150, pp. 258-271, 2018.

[12] A. Dogrul, "Numerical prediction of scale effects on the propulsion performance of Joubert BB2 submarine." *Brodogradnja,* vol. 73, pp. 17-42, Apr 2022.

[13] G. Vaz, S. Toxopeus, and S. Holmes, "Calculation of manoeuvring forces on submarines using two viscous-flow solvers," in *Proceedings of the ASME 2010 29th International Conference on Ocean, Offshore and Arctic Engineering, OMAE2010*. June 6-11, Shanghai, China, 2010.

[14] A. Drouet, et al. *Simulation of submarine manoeuvring using Navier-Stokes solver.* International Conference on Computational Methods in Marine Engineering, MARINE 2011 pp. 301-312, 2011.

[15] Y. Pan, H. Zhang, and Q. Zhou, "Numerical prediction of submarine hydrodynamic coefficients using CFD simulation." *Journal of Hydrodynamics,* vol. 24, pp. 840-847, 2012.

[16] J. T. Zhang, J. A. Maxwell, A. G. Gerber, A. G. L. Holloway, and G. D. Watt, "Simulation of the flow over axisymmetric submarine hulls in steady turning." *Ocean Engineering,* vol. 57, pp. 180-196, 2013.

[17] M. Can, *Numerical Simulation of Hydrodynamic Planar Motion Mechanism Test for Underwater Vehicles.* Master of Science Thesis. Middle East Technical University, Ankara, Turkey, 2014.

[18] S. Duman, S. Sezen, and S. Bal, "Propeller effects on maneuvering of a submerged body," in *3rd International Meeting- Progress in Propeller Cavitation and its Consequences: Experimental and Computational Methods for Predictions,* 15-16 November, Istanbul, Turkey. 2018.

[19] D. Feng, X. Chen, H. Liu, Z. Zhang, and X. Wang, "Comparisons of turning abilities of submarine with different rudder configurations," in *Proceedings of the ASME 2018 37th International Conference on Ocean, Offshore and Arctic Engineering,* June 17-22, 2018, Madrid, Spain.

[20] J. A. Foroushani, and M. Sabzpooshani, "Determination of hydrodynamic derivatives of an ocean vehicle using CFD analyses of synthetic standard dynamic tests." *Applied Ocean Research,* vol. 108, pp. 102539, Mar 2021.

[21] C. Delen, and O. K. Kinaci, "Direct CFD simulations of standard maneuvering tests for DARPA Suboff." *Ocean Engineering,* vol. 276, pp. 114202, May 2023.

[22] E. Kahramanoglu, "Numerical investigation of the scale effect on the horizontal maneuvering derivatives of an underwater vehicle." *Ocean Engineering,* vol. 272, pp. 113883, Mar 2023.

[23] B. Zhao, et al. "Hydrodynamic coefficients of the DARPA SUBOFF AFF-8 in rotating arm maneuver - Part II: Test results and discussion." *Ocean Engineering,* vol. 268, pp. 113466, 2023.

[24] H. Öztürk, K. B. Gündüz, and Y. Arıkan Özden, "Numerical investigation of the maneuvering forces of different darpa suboff configurations for static drift condition." *Journal of ETA Maritime Science,* vol. 11, pp. 137-147, 2023.

[25] A. Tyagi, and D. Sen, "Calculation of transverse hydrodynamic coefficients using computational fluid dynamic approach." *Ocean Engineering,* vol. 33, pp. 798-809, Apr 2006.

[26] A. Phillips, M. Furlong, and S. R. Turnock, The use of Computational Fluid Dynamics to Determine the Dynamic Stability of an Autonomous Underwater Vehicle, 10th Numerical Towing Tank Symposium (NuTTS'07), Hamburg, Germany, 2007.

[27] C. Fureby, et al. "Experimental and numerical study of a generic conventional submarine at10° yaw." *Ocean Engineering,* vol. 116, pp. 1-20, 2016.

[28] P. M. Carrica, M. Kerkvliet, F. Quadvlieg, M. Pontarelli, and J. E. Martin, CFD Simulations and Experiments of a Maneuvering Generic Submarine and Prognosis for Simulation of Near Surface Operation, 31st Symposium on Naval Hydrodynamics Monterey, CA, USA, 2016.

[29] P. M. Carrica, Y. Kim, and J. E. Martin, "Vertical zigzag maneuver of a generic submarine." *Ocean Engineering*, vol. 219, pp. 108386, Jan 2021.

[30] G. Dubbioso, R. Broglia, and S. Zaghi, "CFD analysis of turning abilities of a submarine model." *Ocean Engineering,* vol. 129, 459-479, 2017.

[31] T. T. Nguyen, H. K. Yoon, Y. Park, and C. Park, "Estimation of hydrodynamic derivatives of full-scale submarine using RANS solver." *Journal of Ocean Engineering and Technology,* vol. 32, pp. 386-392, 2018.

[32] H. Kim, D. Ranmuthugala, Z. Q. Leong, and C. Chin, "Six-DOF simulations of an underwater vehicle undergoing straight line and steady turning manoeuvres." *Ocean Engineering,* vol. 150, pp. 102-112, 2018.

[33] S. Zhang, H. Li, T. Zhang, Y. Pang, and Q. Chen, "Numerical simulation study on the effects of course keeping on the roll stability of submarine emergency rising." *Applied Sciences,* vol. 9, pp. 3285, 2019.

[34] R. Doyle, T. L. Jeans, A. G. L. Holloway, and D. Fieger, "URANS simulations of an axisymmetric submarine hull undergoing dynamic sway." *Ocean Engineering*, vol. 172, pp. 155-169, Jan 2019.

[35] Y. J. Cho, W. Seok, K. H. Cheon, and S. H. Rhee, "Maneuvering simulation of an X-plane submarine using computational fluid

dynamics," *International Journal of Naval Architecture and Ocean Engineering,* vol. 12, pp. 843-855, 2020.

[36] K. Han, et al. "Six-DOF CFD simulations of underwater vehicle operating underwater turning maneuvers." *Journal of Marine Science and Engineering,* vol. 9, pp. 1451, Dec 2021.

[37] SNAME, Nomenclature for treating the motion of a submerged body through a fluid, The Society of Naval Architects and Marine Engineers, New York, 1950.

[38] ITTC. 2014. Uncertainty analysis in CFD, verification and validation methodology and procedures, ITTC - Recomm. Proced. Guidelines.

[39] ITTC. 1999. Final report and recommendations to the 22nd ITTC.

[40] P. J. Roache, "Verification of codes and calculations." AIAA Journal. vol. 36, pp. 696-702, May 1998.

[41] F. Stern, R. V. Wilson, H. W. Coleman, and E. G. Paterson, "Comprehensive approach to verification and validation of CFD simulations-Part 1: methodology and procedures." *Journal of Fluids Engineering,* vol. 123, pp. 793-802, Dec 2001.

[42] R. V. Wilson, F. Stern, H. W. Coleman, and E. G. Paterson, "Comprehensive approach to verification and validation of CFD simulations-Part 2: application for rans simulation of a cargo/container ship." *Journal of Fluids Engineering,* vol. 123, pp. 803-810, Dec 2001.

[43] F. Cakici, E. Kahramanoglu, S. Duman, and A. D. Alkan, "A new URANS based approach on the prediction of vertical motions of a surface combatant in head waves." *Ocean Engineering,* vol. 162, pp. 21-33, Aug 2018.

[44] I. B. Celik, U. Ghia, P. J. Roache, C. J. Freitas, and P. E. Raad, "Procedure for estimation and reporting of uncertainty due to discretisation in CFD applications." *Journal of Fluids Engineering,* vol. 130, 078001, Jul 2008.

[45] H. Yoon, C. D. Simonsen, L. Benedetti, J. Longo, Y. Toda, and F. Stern, "Benchmark CFD validation data for surface combatant 5415 in PMM maneuvers - Part I: force/moment/motion measurements." *Ocean Engineering,* vol. 109, pp. 705-734, 2015.

[46] B. Zhao, Y. Yun, F. Hu, J. Sun, D. Wu, and B. Huang, "Hydrodynamic coefficients of the DARPA SUBOFF AFF-8 in rotating arm maneuver - Part I: Test technology and validation." *Ocean Engineering,* vol. 266, 113148, 2022.